SUPPLEMENTARY MATERIAL

Table S1. Inheritance of the *Abcc6* mutation by heterozygous breeding in three mutant rat lines

Mutant line	Gender		Genotype		
	Male	Female	Wt	Het	Hom
SD-*Abcc6*^{em2Qlju} (Line 2):					
Observed	62	62	29	69	26
Expected	62	62	31	62	31
P value	1.000			0.4219	
SD-*Abcc6*^{em3Qlju} (Line 3):					
Observed	55	53	27	52	29
Expected	54	54	27	54	27
P value	0.8474			0.8948	
SD-*Abcc6*^{em4Qlju} (Line 4):					
Observed	74	67	34	70	37
Expected	70.5	70.5	35.25	70.5	35.25
P value	0.5555			0.9348	

Abcc6 heterozygous breeding pairs from three mutant rat lines were maintained on either normal laboratory diet or acceleration diet. Pups were weaned and genotyped at 4 weeks of age. Chi-squared test was used to analyze the comparison of observed and expected distribution; the differences are not statistically significant. Wt, wild type; Het, heterozygous; Hom, homozygous.

FIGURE LEGEND

Figure S1. Quantitative RT-PCR of rat *Abcc6* gene demonstrates expression primarily in the liver and at low levels in the kidney. The amount of *Abcc6* mRNA per sample was normalized to *ACTB* mRNA and expressed relative to the level in the liver (1.0). **(a)** A cDNA panel from 8 rat tissues (liver, kidney, heart, whole brain, spleen, lung, skeletal muscle, and testis) was purchased from Clontech; **(b)** cDNA samples from aorta, skin and eyes were synthesized by the authors. The values are mean of three determinations.

Figure S2. Illustration of targeted mutations in exon 1 of the rat *Abcc6* gene in four rat mutant lines. The ZFN binding site is underlined, and the ZFN cut site is boxed. The mutant lines, SD-*Abcc6*^{em1Qlju} (Line 1), SD-*Abcc6*^{em3Qlju} (Line 3), SD-*Abcc6*^{em4Qlju} (Line 4), *and* SD-*Abcc6*^{em5Qlju} (Line 5), with confirmed germline transmission, carry deletion mutations of 10 bp, 10 bp, 20 bp, and 11 bp, respectively, as indicated in the figure. These deletion mutations are predicted to cause out-of-frame translation and premature stop codon.

Figure S3. Energy dispersive X-ray analysis of the mineral deposits in the dermal sheath of vibrissae reveals hydroxyapatite deposition. Elemental composition analysis in mineralized area reveals the presence of calcium and phosphorus as the principal ions in 1.57:1 atomic ratio (**a**). The presence of carbon (c) reflects the carbon coating of the sample. X-ray topography of the distribution maps of calcium (**b**, red) and phosphorus (**c**, green) reveals co-localization, as demonstrated by merging the calcium and phosphorus maps (**d**).

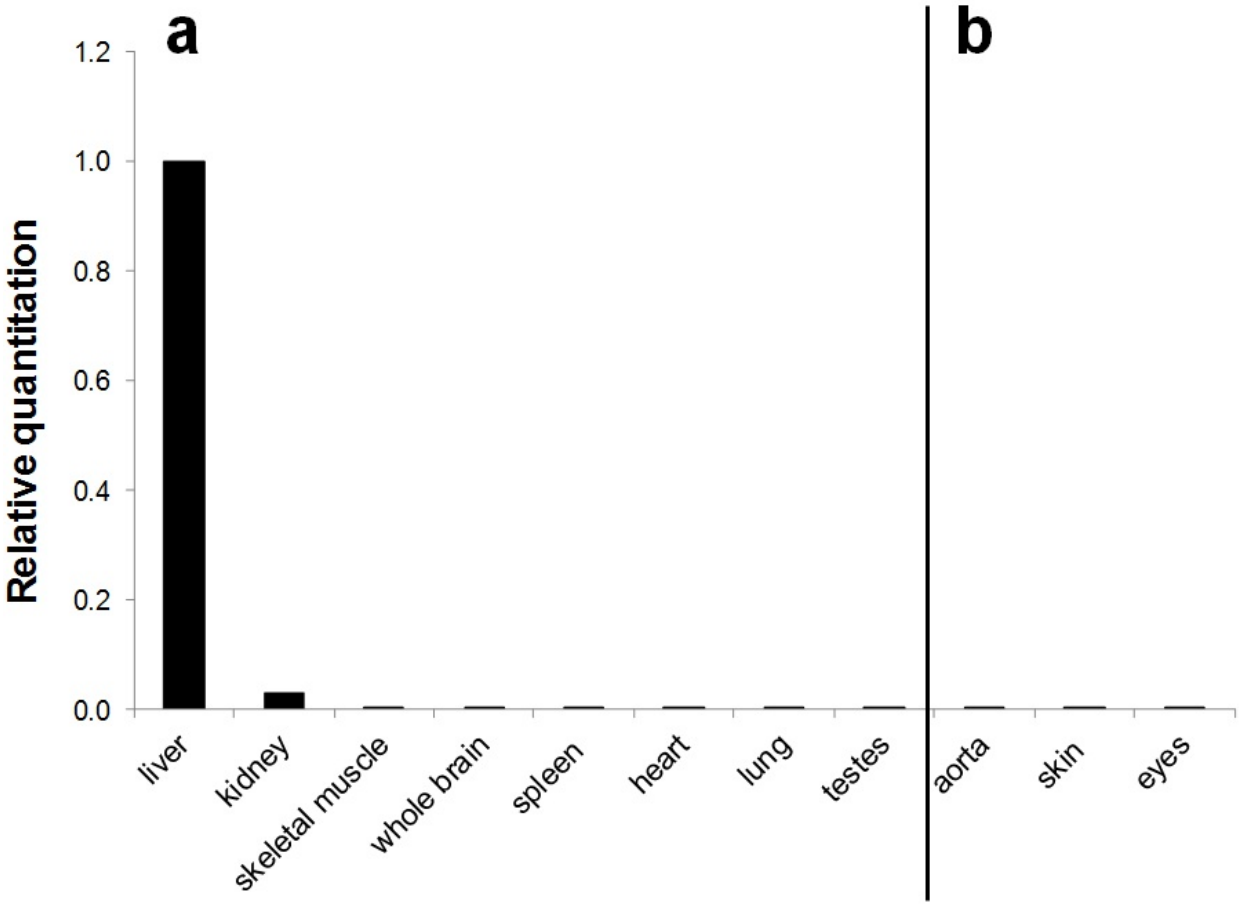
a
b
Relative quantitation
1.2
1.0
0.8
0.6
0.4
0.2
0.0
liver
kidney
skeletal muscle
whole brain
spleen
heart
lung
testes
aorta
skin
eyes

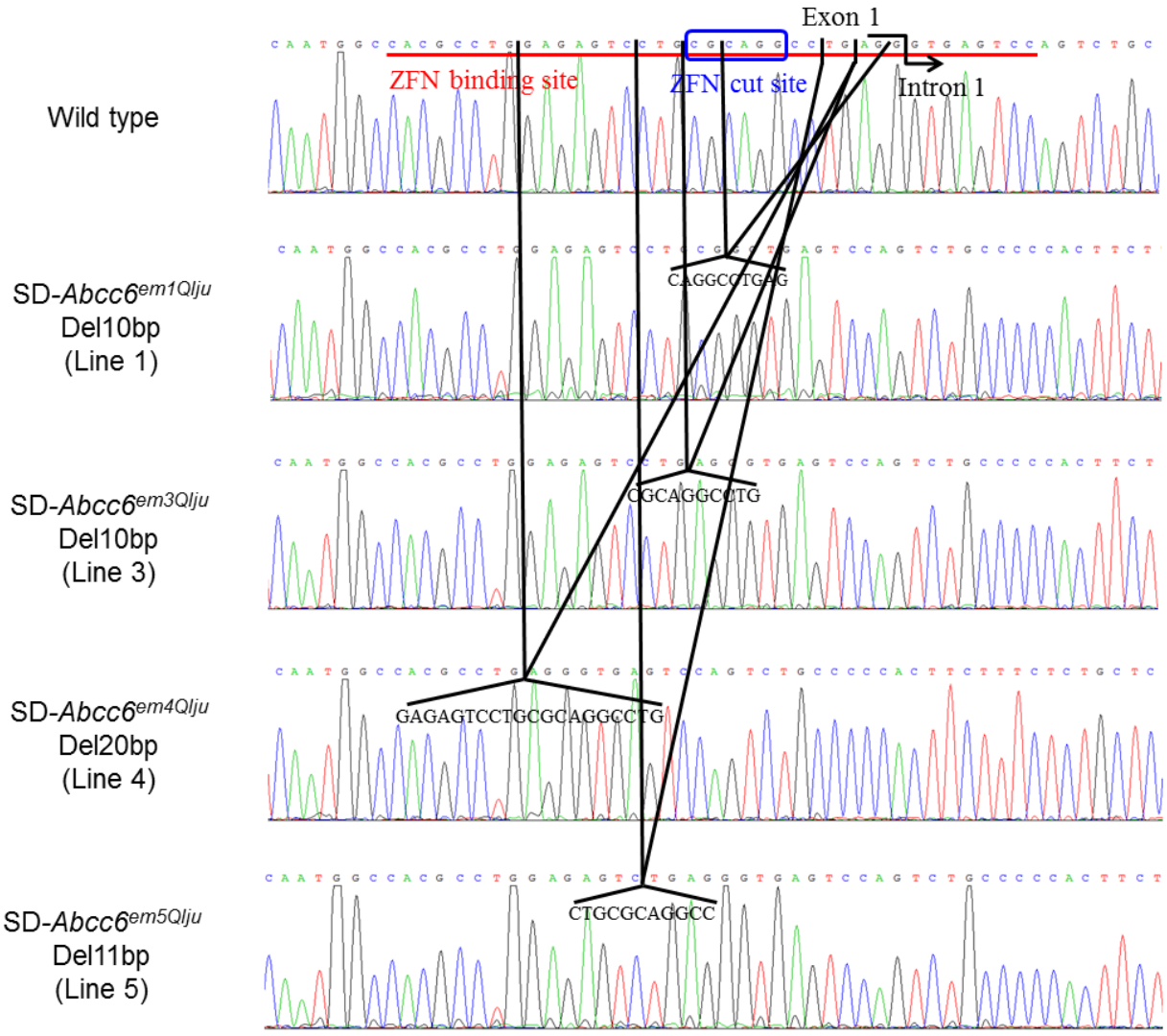
Exon 1
ZFN binding site
ZFN cut site
Intron 1
Wild type
SD-Abcc6em1Qlju
Del10bp
(Line 1)
CAGGCCTGAG
SD-Abcc6em3Qlju
Del10bp
(Line 3)
CGCAGGCCTG
SD-Abcc6em4Qlju
Del20bp
(Line 4)
GAGAGTCCTGCGCAGGCCTG
SD-Abcc6em5Qlju
Del11bp
(Line 5)
CTGCGCAGGCC

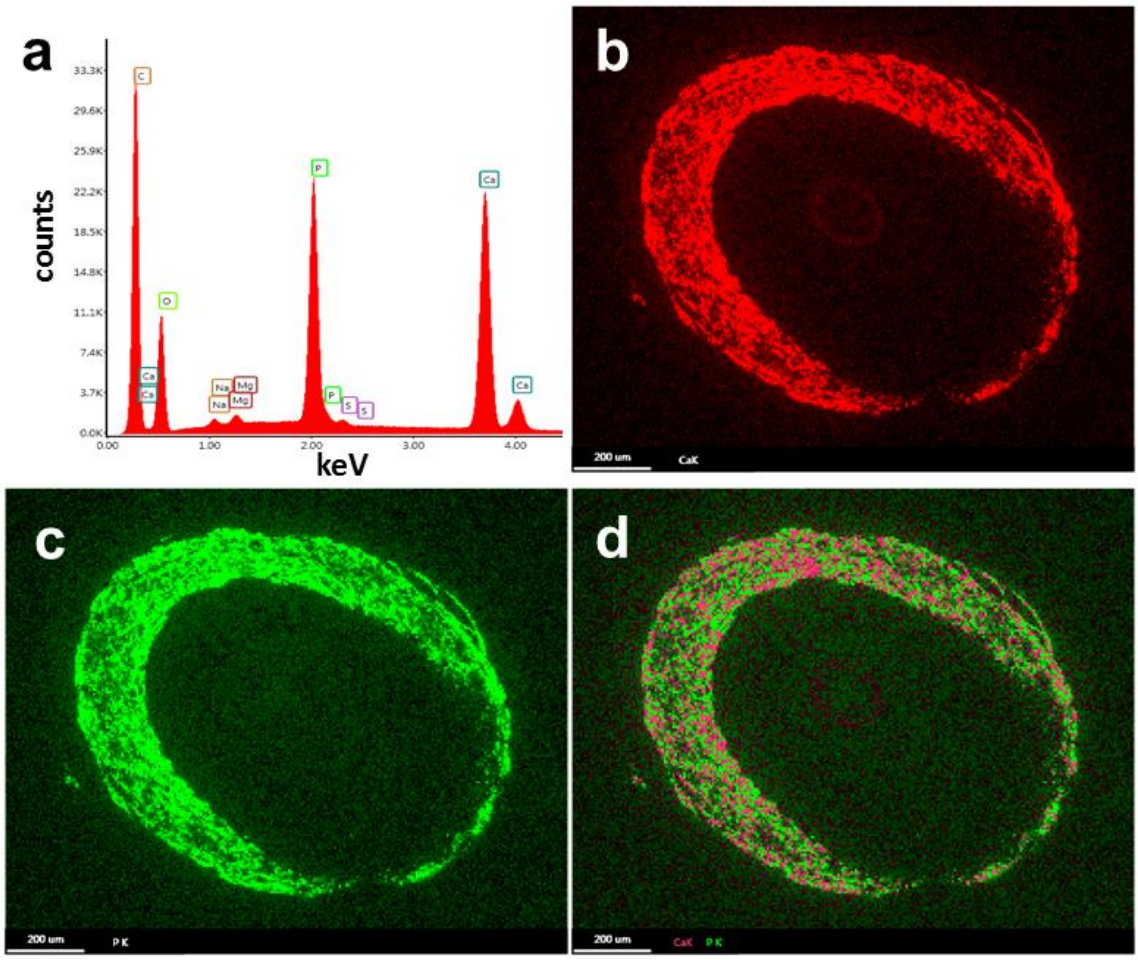
a
counts
keV
C
O
Ca
Ca
Na
Mg
Na
Mg
P
S
S
Ca
Ca
b
200 um
CaK
c
200 um
P K
d
200 um
CaK
P K